Alignment aberrations of the New Solar Telescope

Anastacia M. Manuel and James H. Burge

College of Optical Sciences/University of Arizona
1630 East University Blvd., Tucson, AZ 85721, USA

ABSTRACT

The New Solar Telescope (NST) is an off-axis Gregorian telescope at Big Bear Solar Observatory (BBSO). This paper presents the expected aberrations due to misalignments of the secondary mirror for a general Gregorian telescope using an optical model of the on-axis "parent" telescope version of NST. The sensitivities of linear astigmatism and constant coma found by perturbing the axisymmetric model are presented and shown to match those predicted by the theory. Then we discuss how the actual aberrations are different due to the off-axis nature of the NST. Finally, we discuss the effect of the misalignments on the pointing of the telescope.

Keywords: Aberrations, Off-axis telescope, Alignment

1. INTRODUCTION

The aberrations due to misalignment of the secondary mirror in the New Solar Telescope (NST) are reviewed in this publication. The New Solar Telescope (NST) is an off-axis Gregorian telescope at Big Bear Solar Observatory (BBSO).[1] The telescope will operate in the wavelength range of 390 nm into the far infrared. The design of the telescope is presented in Section 1.1. Section 2 includes a discussion of the aberrations due to misalignments of the secondary mirror for a general on-axis Gregorian telescope with the same first order properties as NST. The observed aberrations of constant coma and linear astigmatism for this "parent" telescope from the ZEMAX model match what is expected in a misaligned telescope. Section 3 includes a discussion of the changes to the observed aberrations due to the off-axis nature of the NST. Finally, Section 4 discusses the effect of the misalignments on the pointing of the telescope.

1.1 Optical Design of the New Solar Telescope

The New Solar Telescope is an off-axis telescope with the same design parameters (e.g. radii, conic constants) as a theoretical on-axis parent telescope, but only certain off-axis sections of the theoretical on-axis telescope are fabricated and used. The reasons for the off-axis design, discussed in detail by Didkovsky,[1] are to avoid having a central obscuration and spiders. The primary and secondary mirrors (M1 and M2) of NST together compose a Gregorian telescope and then either one or two flat fold mirrors (M3 and M4) are used to send the light to either the Nasmyth or Gregory-Code focal plane. The two mirror system prescription is listed in Table 1.

Table 1: NST system prescription

Surface Name	Radius of curvature (mm)	Conic constant	Thickness (mm)
M1	-7700	-1	3850
Prime Focus			300.05
M2	573.5828	-0.83087	6490.259
Gregorian Focus			

The (off-axis) primary mirror (f/2.4) has a radius of curvature of 7700 mm and a clear aperture diameter of 1600 mm, as shown in the telescope design in Fig. 1a. This mirror was figured and tested at the University of Arizona as a 1/5 scale demonstration[2] for the 8.4 m diameter off-axis mirror segments of the 25 m f/0.7 Giant

Further author information:
A.M.M.: E-mail: amh21@email.arizona.edu, Telephone: 1 520 626 6826
J.H.B.: E-mail: JBurge@optics.arizona.edu, Telephone: 1 520 621 8182

Magellan Telescope (GMT)[3] primary. For simplification during the analysis of the off-axis telescope, the two fold mirrors were removed, as in Fig. 1b. To make the axisymmetric parent telescope of NST in ZEMAX, the coordinate breaks and off-axis aperture definitions were removed, as shown in Fig. 1c. The aperture stop is the primary mirror and a comparison of the two pupils is shown in Fig. 1d—the end view of the optical design.

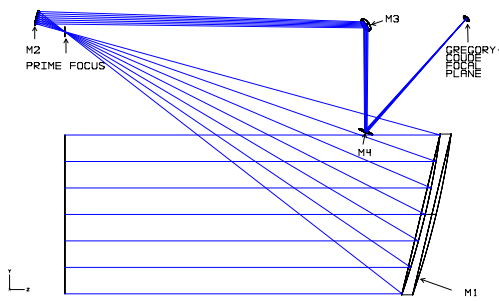

(a) NST with all four mirrors (f/52.05 system)

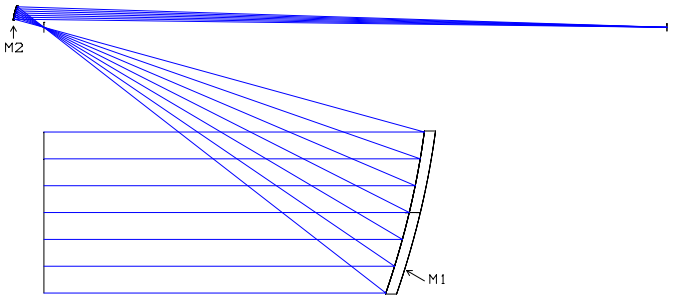

(b) NST after fold mirrors removed (f/52.05 system)

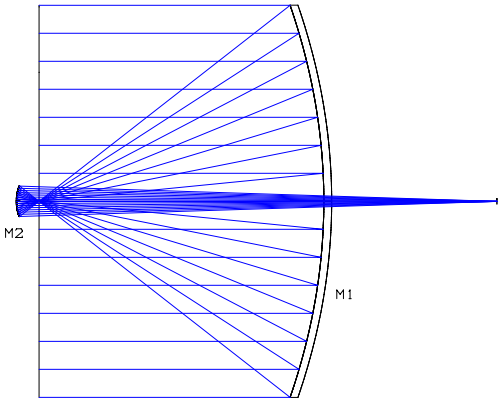

(c) Side view of NST on-axis parent telescope (f/15.77 system)

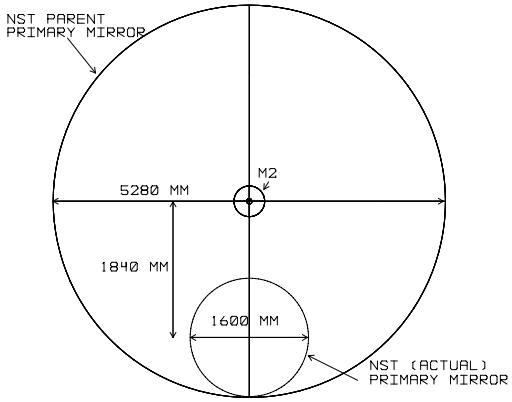

(d) End view of the two pupils

Figure 1: New Solar Telescope optical layout. The f/number calculations are provided in the appendix (Section 6).

2. ABERRATIONS OF THE PARENT ON-AXIS GREGORIAN TELESCOPE

The analysis in this paper assumes that all the optics are made perfectly and that the only aberrations beyond the residual aberrations are introduced by rigid body misalignments of those optics. (The residual design aberrations are those that exist in the optical model, since it is impossible to design a system to be absolutely perfect.) The image quality of a two mirror telescope is dependent on the position of the secondary mirror relative to the primary mirror. The position of the primary mirror, which serves as the reference, only affects the pointing of the telescope. As for any object, the secondary mirror has six rigid body degrees of freedom as defined from the surface vertex: $\vec{x}$, $\vec{y}$, and $\vec{z}$ rotations; and $\vec{x}$, $\vec{y}$, and $\vec{z}$ translations. The first two degrees of freedom for the secondary mirror may be defined as: 1. rotation about the optical axis, which has no effect in a rotationally symmetric system and 2. translation of the secondary along the optical axis, which only causes defocus and a small amount of spherical aberration. These degrees of freedom will not be further discussed in this paper because their effect on system performance is decoupled from the remaining non-axisymmetric degrees of freedom, which are the emphasis of the paper. The other four degrees of freedom (two tilts and two decenters) of the secondary mirror will each individually cause both coma and astigmatism where the sign of the aberration depends on the direction of the misalignment and the amount depends on the magnitude of the perturbation. Other higher

order aberrations may occur in addition to third order coma and astigmatism, but are not significant in a system without too many degrees of freedom.

However, it is possible to define the degrees of freedom differently such that the $\vec{x}$ and $\vec{y}$ translations and rotations about the vertex are combined into rotations about two different points along the optical axis. Different linear combinations of rotations about these points can achieve any of the same vertex rotations plus translations as before. In a two-mirror telescope, there is a point on the optical axis where rotations about this point do not introduce any coma.[4–6] This "coma-free point" or "neutral point" exists because different misalignment degrees of freedom produce the same types of aberrations with different magnitude ratios. Thus, it is possible to cancel the coma introduced by a decenter with the coma that is introduced by a tilt that it is properly chosen. This linear combination of tilt and decenter is equivalent to a rotation about the coma-free point and since the effect on the aberration of a perturbation is linear, the coma is always balanced for any rotation angle of the secondary mirror about the coma-free point. However, rotations about this coma-free point still introduce field astigmatism. The coma-free point for a classical telescope such as this is at the focus of the primary mirror and for more complex systems, the position of the coma-free point can be found using the equations in the references[4,5] or a lens design program. (This point will be abbreviated PF for prime focus in the figures and tables below.) In NST, the prime focus is located 300.1 mm away from the vertex of the secondary mirror, as shown in Fig. 2a.

In a classical telescope, the primary mirror is a paraboloid (conic constant $k = -1$). The type of telescope is defined by whether the secondary mirror is concave (Gregorian) or convex (Cassegrain). In a Gregorian telescope, the secondary mirror is an oblate ellipsoid ($-1 < k < 0$) such that one focus of the ellipse is at the prime focus and the other is at the system focal plane. The two foci are conjugate points and the light rays can transfer perfectly from one focus to the other focus according to Fermat's Principle. As the secondary mirror ellipsoid rotates about the prime focus (one of its focal points), the rays for the on-axis field that go through the prime focus on the optical axis still can form a perfect image at the other focal point (the system focus). However, as the field angle increases, the aberrations increase.

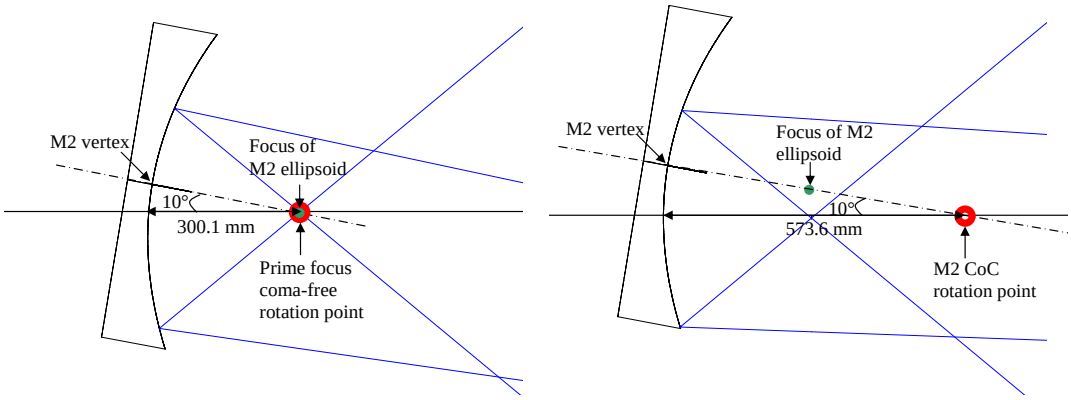

(a) Rotation about PF (b) Rotation about M2 CoC

Figure 2: M2 degrees of freedom. (The rotations are shown larger than would actually occur to clearly show the location of the rotation point.)

A spot diagram for NST with M2 having some rotation about the coma-free point is shown in Fig. 3a. This spot diagram shows astigmatism, which causes the focused spots to be elongated. At the sagittal and tangential image planes, the images would form perfect line images. In particular, the astigmatism shown here has a linear field dependence, which can be seen by the length of the spots throughout the field and the particular orientation pattern of the elongated spots throughout the field. For the large rotation angle used in Fig. 3a, the pointing error would be very large, so it is not included in the spot diagram.

Specifying $\vec{x}$ and $\vec{y}$ rotations about the coma-free point uses two degrees of freedom. The remaining two degrees of freedom may either be regular vertex tilts or decenters or a combination that results in rotation

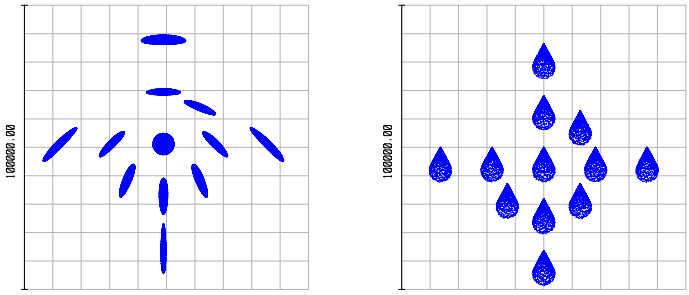

(a) M2 rotated about coma-free point (PF) showing linear astigmatism ($PFRotX = 5.5°$).

(b) M2 rotated about neutral point for pointing (M2 CoC) showing constant coma ($CoCRotX = 0.1°$).

Figure 3: Effect of M2 degrees of freedom on spot diagrams. The maximum field angle spots are shown for a full field of view of 3 arcminutes. Spot sizes are exaggerated by 4× for clarity. (These spot diagrams are what you would see looking toward the focal plane, and not from behind it.)

about another point on the axis. For this paper, we will define the final two degrees of freedom as $\vec{x}$ and $\vec{y}$ rotations of the secondary mirror about its center of curvature (CoC). Perturbing this degree of freedom results the aberrations of constant coma and linear astigmatism, however it does not result in a pointing error for the paraxial rays. In NST, the CoC of the secondary mirror is located 573.6 mm away from the vertex of the secondary mirror, as shown in Fig. 2b. The center of curvature of the secondary mirror is always a pointing-free neutral point (no matter what the shape of the secondary is).[4] This can be visualized by considering the case of a spherical secondary mirror. For this case, rotations about the center of curvature have absolutely no effect on the shape of the optical surface. The paraxial rays which do not have a pointing error in Fig. 3b are those at the pointed tip of the coma pattern. (Comatic images are identified by their teardrop or comet shape.) Since the coma aberration causes a nonsymmetric image blur, the centroid pointing does indeed change for center of curvature rotations. If desired, a lens design program could be used to find an alternate rotation point that does not cause centroid pointing errors. This point would be near the M2 center of curvature, but slightly displaced along the optical axis.

The definition of these degrees of freedom for the secondary mirror is a convenient choice because it decouples the effects of coma and pointing. Table 2 summarizes the results that a rotation of the secondary mirror about the coma-free point will only introduce astigmatism and a pointing change, while a rotation of the secondary about its center of curvature causes no pointing error, but introduces both constant coma and linear astigmatism. The name of the aberration (i.e. coma or astigmatism) describes the shape of the wavefront in the exit pupil while the preceding modifier (i.e. constant or linear) describes the magnitude of the aberration as a function of the field of view.

Table 2: Summary of the secondary mirror degrees of freedom and effects on aberrations

Rotation point for secondary mirror	**Prime Focus** (neutral point for coma or coma-free point)	**M2 Center of Curvature** (neutral point for pointing)
Distance from M2 vertex	300.1 mm	573.6 mm
Aberrations:		
Constant coma	No	Yes (dominating effect)
Linear astigmatism	Yes	Yes (but small effect)
Pointing change	Yes	No

2.1 Using aberrations for aligning the system

Knowledge of the aberrations and their sensitivities to misalignment can be used to align an optical system. In a two mirror telescope, one can rotate the secondary mirror about its center of curvature until the constant coma is eliminated, then rotate the secondary about the prime focus (coma-free point) until the linear astigmatism is gone. This rotation about prime focus will also simultaneously eliminate pointing errors, which alternatively may be easier to measure and correct. Pointing errors are discussed in Section 4.

It is interesting to note that if the primary mirror surface is incorrectly figured with coma, the telescope images during operation will appear with the same constant coma as that caused by a secondary mirror misalignment. This means that some amount of coma figure error on the primary can be accommodated by purposely misaligning the telescope without any degradation in performance. Similarly, if the primary mirror is incorrectly figured with astigmatism, this astigmatism will show up equally for all field angles. However, this constant astigmatism can not be corrected by purposely misaligning the secondary mirror because the astigmatism due to misalignment has linear field dependence. Thus, the astigmatism error in the mirror shape must be corrected by other means, such as additional polishing or by bending the surface with active supports during operation.

The telescope alignment adjustments can be calculated if the sensitivities of the secondary mirror to misalignments are known from the optical model. The sensitivities of the aberrations that arise with a tilted or decentered secondary mirror are described using Zernike polynomial coefficients in this section. This description is based on the work of Tessieres[7,8] and Thompson.[9,10] A similar alignment problem was described for the prime focus corrector of the Bok 90-inch telescope on Kitt Peak by Tessieres.[11] In this paper, we store the information in a matrix which relates the Zernike coefficients to the perturbations. In a system with only two elements, tilt and decenter perturbations only cause primary coma and astigmatism, which are represented by the coefficients C_5–C_8 for the standard Zernike polynomials in Z_5–Z_8. We use the standard Zernike definitions described by Noll[12] where subscripts 5 and 6 correspond to astigmatism, while 7 and 8 correspond to coma. (It is assumed that a separate procedure will be used to focus the telescope and set the secondary mirror spacing to eliminate focus (Z_4) and spherical aberration (Z_{11}).) Therefore, a 4×4 reconstructor matrix $\boldsymbol{M}$ with components $m_{ij}(1 \le i \le 4, 1 \le j \le 4)$ is sufficient to describe the alignment aberrations:

$$\begin{bmatrix} C_5 \\ C_6 \\ C_7 \\ C_8 \end{bmatrix} = \begin{bmatrix} m_{11} & m_{12} & m_{13} & m_{14} \\ m_{21} & m_{22} & m_{23} & m_{24} \\ m_{31} & m_{32} & m_{33} & m_{34} \\ m_{41} & m_{42} & m_{43} & m_{44} \end{bmatrix} \cdot \begin{bmatrix} PFRotX \\ PFRotY \\ CCRotX \\ CCRotY \end{bmatrix}. \tag{1}$$

In a system that has more elements which may be perturbed, there should be additional columns in $\boldsymbol{M}$ for each degree of freedom. These extra degrees of freedom cause additional aberrations to become significant and therefore, more rows would be required. Eq. 1 can also be written in shortened form as $Z = \boldsymbol{M}A$ where Z is the vector of Zernike coefficients C_5–C_8 and A is a vector storing the alignment perturbations. When the reconstructor matrix $\boldsymbol{M}$ and the specific Zernike aberration coefficients C_5–C_8 are known, a least-squares fit can be used to determine the current misalignments using the equation $A = \boldsymbol{M}^{-1}Z$. The system can then be aligned once the amounts of the misalignments are calculated.

In principle, the Zernike aberrations can be measured for one position in the field and the misalignments can be calculated; however in a real system, noise prevent accurate calculations of the perturbations. Thus, a least-squares fit with multiple measurements in the field will be used to minimize the effects of the noise. To do this, extra rows are added to the vectors and matrices in Eq. 1;

$$Z_{4n\times 1} = \boldsymbol{M}_{4n\times 4}A_{4\times 1} \tag{2}$$

where n is the number of field points. The aberrations that can occur due to misalignments may only have certain field dependencies and these must be known in order to fill the $\boldsymbol{M}$ matrix. The field dependencies have been described by Thompson for third and fifth order Seidel aberrations[9,10] and by Tessieres for Zernike polynomials.[7] In this paper, we fit coefficients to the equations describing the field dependencies of the Zernikes as found by Tessieres.

2.2 Field-dependent Zernike aberrations in a misaligned system

Typically, a single wavefront $W(\rho, \phi)$ can be described by a sum of scaled Zernike polynomials:

$$W(\rho, \phi) = \sum_i C_i Z_i(\rho, \phi) \tag{3}$$

where C_i is the weighting coefficient of the Zernike polynomial $Z_i(\rho, \phi)$. However one might also describe the wavefront for any field angle in a system by making the weighting coefficients field-dependent functions $C_i(x, y)$ and Eq. 3 becomes:

$$W(\rho, \phi, x, y) = \sum_i C_i(x, y) Z_i(\rho, \phi). \tag{4}$$

A complete set of equations have been developed to describe the Zernike polynomials in a misaligned system.[8] In the previous section, it was shown that constant coma and linear astigmatism are the dominant aberrations caused by misalignments in a two-mirror optical system. The following equations express the field-dependent Zernike coefficients of astigmatism (Z_5 and Z_6) and coma (Z_7 and Z_8) in a misaligned system:

$$C_5(x, y) = \alpha_0(y^2 - x^2) - \alpha_1 x + \alpha_2 y + \alpha_4 \tag{5}$$
$$C_6(x, y) = 2\,\alpha_0 x\, y + \alpha_1 y + \alpha_2 x + \alpha_3 \tag{6}$$
$$C_7(x, y) = \beta_0 y + \beta_2 \tag{7}$$
$$C_8(x, y) = \beta_0 x + \beta_1. \tag{8}$$

In Eq. 5 and 6, we see that the total astigmatism can be a combination of astigmatism components that are quadratic, linear and constant in field, while in Eq. 7 and 8, we see coma can be linear or constant in field. Eqs. 5-8 can also be expressed in a matrix format:

$$\begin{bmatrix} C_5 \\ C_6 \\ C_7 \\ C_8 \end{bmatrix} = \begin{bmatrix} (y^2 - x^2) & -x & y & 0 & 1 & 0 & 0 & 0 \\ 2xy & y & x & 1 & 0 & 0 & 0 & 0 \\ 0 & 0 & 0 & 0 & 0 & y & 0 & 1 \\ 0 & 0 & 0 & 0 & 0 & x & 1 & 0 \end{bmatrix} \cdot \begin{bmatrix} \alpha_0 \\ \alpha_1 \\ \alpha_2 \\ \alpha_3 \\ \alpha_4 \\ \beta_0 \\ \beta_1 \\ \beta_2 \end{bmatrix}. \tag{9}$$

Eq. 9 corresponds to one column of $\boldsymbol{M}$. The Greek letter coefficients with subscript $n = 0$ correspond to aberrations that occur in a rotationally symmetric system.[7,8]

2.3 Effect of misalignments on aberrations (Finding the reconstructor matrix)

The optical model used in this section is the NST axisymmetric parent telescope, described in Section 1.1. The specific aberrations in the actual off-axis NST will be different, but it is important to first show the technique that will be used. Each column of the matrix $\boldsymbol{M}$ shown in Eq. 1 corresponds to a perturbation of one alignment degree of freedom for the secondary mirror. The columns are calculated one at a time (left to right), starting with a coma-free (prime focus) rotation about $\vec{x}$, then about $\vec{y}$, then pointing-free (CoC) rotation about $\vec{x}$ and then about $\vec{y}$. The process of finding the aberrations in ZEMAX consists of the following steps for each misalignment perturbation.

1. Record the Zernike coefficients at a grid of field angles for some amount of perturbation. (The size of the perturbation can be arbitrarily chosen, as long as it is in the regime where it has a linear effect on the aberration coefficients.)

2. Perform a least-squares fit on the recorded Zernike coefficients to the find the coefficients α_0-α_3 and β_0-β_2 that describe each degree of freedom.

2.3.1 Record the Zernike coefficients throughout the field for perturbations of M2

The first step in the process of finding the equations which relate the Zernike coefficients to the perturbations is to perturb the secondary mirror with a significant amount of rotation. For each perturbation, the Zernike coefficients are recorded for a grid of 50 different field positions using a ZEMAX macro. The Zernike coefficients are then stored in five separate data files for: 1. the nominal system, 2. the secondary mirror PF $\vec{x}$ rotation, 3. the secondary mirror PF $\vec{y}$ rotation, 4. the secondary mirror $\vec{x}$ CoC rotation and 5. the secondary mirror $\vec{y}$ CoC rotation. The residual design aberrations of the nominal system are recorded, so the effect of the misalignment can be found by taking a difference between the coefficients before and after the misalignment is applied.

Rotating the secondary mirror about the coma-free point (the prime focus) results in linear astigmatism, as shown by the spot diagrams in Fig. 4. As mentioned earlier, linear astigmatism always has this pattern of line images throughout the field. However the pattern for the entire field rotates by 90°, depending on the direction of the rotation of M2. (The orientation angle of the line image for any field angle may be calculated and is 1/2 the arctangent of the ratio of the Zernike coefficients C_5 and C_6.[7]) Errors in this degree of freedom are tolerable because the astigmatism grows linearly from the on-axis field and therefore small field angles have small aberrations. In Fig. 4, a rather large rotation angle of 5.5° is used, so that the induced linear astigmatism is clearly shown over the residual field curvature in the design. This large misalignment causes a large amount of pointing error, so the spots in Fig. 4 are shown as referenced to the centroid.

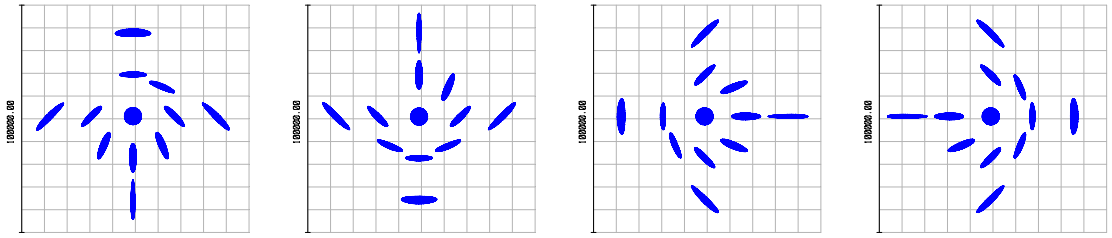

(a) Positive $\vec{x}$ rotation (b) Negative $\vec{x}$ rotation (c) Positive $\vec{y}$ rotation (d) Negative $\vec{y}$ rotation

Figure 4: Spot diagrams of NST with M2 rotated about prime focus by 5.5° showing linear astigmatism. The full field of view is 3 arcminutes. Spot sizes are exaggerated by 4× for clarity.

Rotating the secondary mirror about its CoC causes mostly constant coma, as seen in Fig. 5. The direction of the coma pattern depends on the axis and direction of rotation. This secondary mirror perturbation also causes a small amount of astigmatism compared to the coma, but it is not visible in the figure. Notice that the tip of the coma pattern for the on-axis field is centered in the field, so there is no pointing error. The rotation angle for Fig. 5 is much smaller than the rotation about prime focus in the Fig. 4, but the spot size exaggeration is the same, so the amount of coma is very large. Since this misalignment causes so much coma, it is an important degree of freedom to correct, especially since it affects all field angles equally.

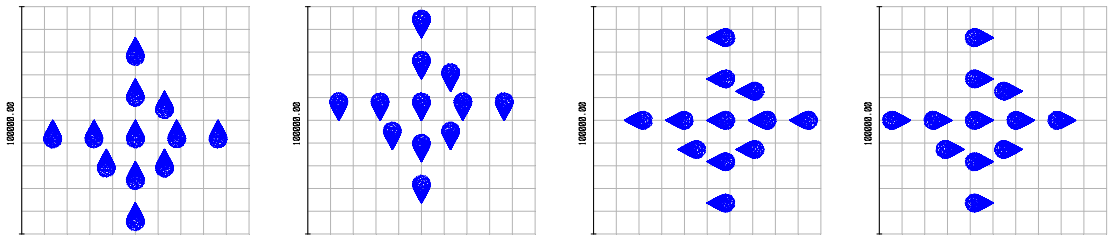

(a) Positive $\vec{x}$ rotation (b) Negative $\vec{x}$ rotation (c) Positive $\vec{y}$ rotation (d) Negative $\vec{y}$ rotation

Figure 5: Constant coma caused by rotating the secondary mirror about its center of curvature by 0.1°. The full field of view is 3 arcminutes. Spot sizes are exaggerated by 4× for clarity.

2.3.2 Perform a least-squares fit to find the values of α_n and β_n

To find the equations which relate the Zernike coefficients to the perturbations and the field positions, a least-squares fit is performed on the recorded data using a MATLAB script. For each perturbation, the script finds the values of all the α_n and β_n terms to describe the field dependent Zernike coefficients. The results are listed in Table 3. One of the linear astigmatism coefficients (α_1 or α_2) are significant for all the degrees of freedom, as expected. The center of curvature rotations have a significant amount of constant coma (β_1 or β_2) and a small amount of constant astigmatism (α_3). All other terms are essentially zero, but are left in the table to show their relative sizes from the numerical fit.

Table 3: α and β coefficients for rotations of 1°

Aberration		$PFRotX$	$PFRotY$	$CoCRotX$	$CoCRotY$
Quadratic astigmatism	α_0	-1.9×10^{-4}	-2.8×10^{-4}	2.8×10^{-3}	-3.0×10^{-4}
Linear astigmatism	α_1	-56.13	-6.7×10^{-7}	-51.72	5.0×10^{-5}
Linear astigmatism	α_2	-1.7×10^{-5}	-56.13	-5.5×10^{-5}	-51.72
Constant astigmatism	α_3	-2.5×10^{-4}	2.5×10^{-4}	3.72	-3.72
Constant astigmatism	α_4	-2.2×10^{-7}	-6.2×10^{-8}	4.5×10^{-6}	-6.5×10^{-7}
Linear coma	β_0	-5.4×10^{-3}	-3.5×10^{-3}	8.3×10^{-2}	9.5×10^{-2}
Constant coma	β_1	-1.1×10^{-5}	-4.9×10^{-3}	-2.1×10^{-4}	39.52
Constant coma	β_2	4.9×10^{-3}	-8.7×10^{-7}	-39.52	-2.1×10^{-5}

2.4 Summary of least squares fit coefficients

Finally, the Zernike coefficients can be expressed in terms of the perturbations and the field positions in the matrix form (now ignoring the almost-zero terms):

$$\begin{bmatrix} C_5 \\ C_6 \\ C_7 \\ C_8 \end{bmatrix} = \begin{bmatrix} 56.13x & -56.13y & -51.72x & -51.72y \\ -56.13y & -56.13x & 51.72y + 3.72 & 51.72x - 3.72 \\ 0 & 0 & -39.53 & 0 \\ 0 & 0 & 0 & -39.53 \end{bmatrix} \cdot \begin{bmatrix} PFRotX \\ PFRotY \\ CoCRotX \\ CoCRotY \end{bmatrix} \tag{10}$$

where x and y are the field angles in degrees, the Zernike coefficients are in nanometers, and the misalignment rotations are in degrees.

3. ABERRATIONS OF NST (THE ACTUAL OFF-AXIS TELESCOPE)

The analysis done in Section 2 was performed for the full NST parent telescope, however the actual NST will just be an off-axis portion of the entire telescope. Using convenient MATLAB codes written by Lundström,[13] the Zernike coefficients of one circular (or elliptical) pupil can be converted into coefficients of another scaled, translated, or rotated pupil. The coefficients of the Zernike polynomials in the subpupil only contain lower orders than the Zernike coefficients originally placed on the pupil. Table 4 shows how one unit of an aberration in the NST parent pupil transforms into lower order aberrations for the actual NST pupil.

As we saw earlier, constant coma is caused by rotating the secondary mirror about any point other than the prime focus. The degree of freedom used in this paper was the M2 center of curvature. The wavefronts in Fig. 6 shows conceptually how coma over the parent telescope pupil transforms into astigmatism and coma (once piston, tip, tilt and focus are removed) for the NST pupil (a subaperture of the larger pupil) according to the values in Table 4.

Since aberrations on one larger pupil only transform to aberrations of a lower order on a subaperture, astigmatism (Z_5 or Z_6) transforms into Zernike terms 1-6. However, if piston and tilt are once again removed, then only astigmatism remains (similar to the case of coma). As another example, shown in Fig. 7, one unit of Z_5 astigmatism on the full aperture looks like -0.5173 units of Z_2 coma and 0.0918 units of Z_5 astigmatism on the subaperture.

Table 4: Conversion of Zernike Polynomials to Lower Order for NST Pupil

Aberration in off-axis portion		Astigmatism $Z_5 = 1$	in parent $Z_6 = 1$	Coma $Z_7 = 1$	in parent $Z_8 = 1$
Piston	Z_1	0	-1.1899	0.5268	0
Tilt	Z_2	-0.5173	0	0	-0.1539
Tilt	Z_3	0	0.5173	1.0952	0
Focus	Z_4	0	0	-0.3135	0
Astigmatism	Z_5	0.0918	0	0	-0.2217
Astigmatism	Z_6		0.0918	0.2217	0
Coma	Z_7			0.0278	0
Coma	Z_8				0.0278

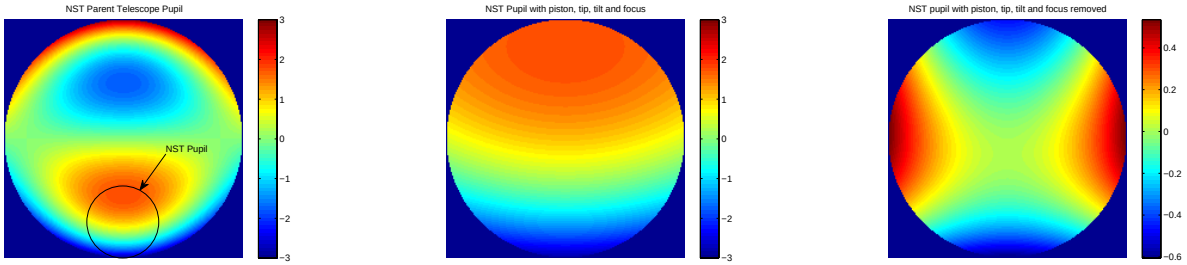

(a) Coma in the full aperture of the parent telescope ($Z_7 = 1$)

(b) Coma over subaperture, the actual NST aperture ($Z_7 = 0.028$, $Z_6 = 0.222$, $Z_4 = -0.314$ $Z_3 = 1.095$, $Z_1 = 0.5268$)

(c) Coma over subaperture (Actual NST aperture), piston and tilt removed ($Z_7 = 0.028$, $Z_6 = 0.222$)

Figure 6: Transformation of 1 unit of coma from NST parent telescope pupil to actual pupil

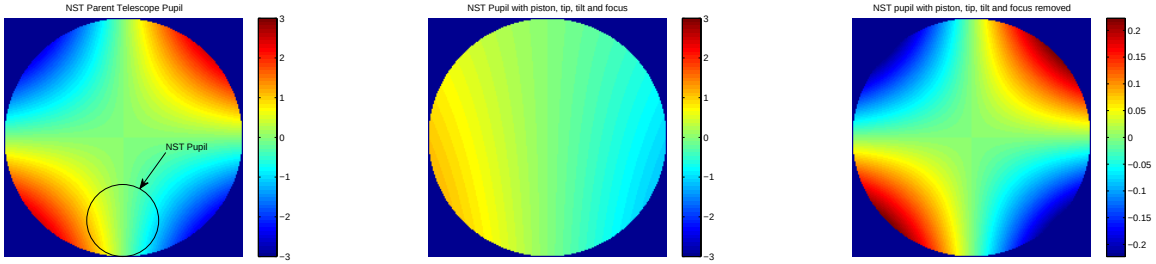

(a) Astigmatism in the full aperture of the parent telescope ($Z_5 = 1$ unit)

(b) Astigmatism over subaperture, the actual NST aperture ($Z_5 = 0.092$ unit, $Z_2 = -0.517$ unit)

(c) Astigmatism over subaperture (Actual NST aperture), piston and tilt removed ($Z_5 = 0.092$ unit)

Figure 7: Transformation of 1 unit of astigmatism over NST parent telescope pupil and actual pupils

Table 5 shows conceptually how the dominant aberrations that occur for the misaligned parent telescope transform into different aberrations for the off-axis NST, following the results in Table 4.

Next, we observe the spot diagrams for the off-axis NST telescope. The degrees of freedom used are exactly the same as those used for the parent telescope. Fig. 8 shows the spot diagrams for rotations about the prime focus for the off-axis NST telescope. Here, the secondary mirror is rotated by the same angle and the spot size exaggeration is the same, so these figures may be directly compared to those in Fig. 4. The rays in this figure are exactly a subset of the rays in the Fig. 4. Since normally prime focus rotations result in mostly linear astigmatism, we should expect that in the off-axis system, the aberrations will include a linear astigmatism and a plate scale change, according to Table 5. This is indeed what we see in Fig. 8.

Table 5: Comparison of aberrations for on-axis and off-axis telescopes

On-axis parent telescope	Off-axis telescope
Constant coma	Constant coma
	Constant astigmatism
	Constant tilt (pointing)
	Constant focus (defocus)
Linear astigmatism	Linear astigmatism
	Linear tilt (plate scale change)
Pointing	Pointing

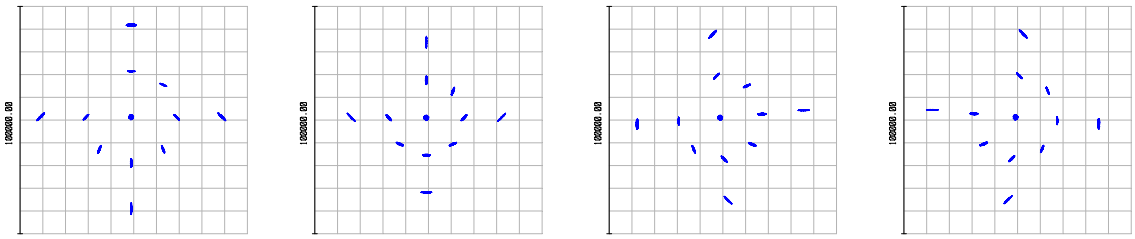

(a) Positive $\vec{x}$ rotation (b) Negative $\vec{x}$ rotation (c) Positive $\vec{y}$ rotation (d) Negative $\vec{y}$ rotation

Figure 8: Spot diagrams when secondary mirror is rotated about the focus of the primary mirror 5.5°. The full field of view is 3 arcminutes. The spot size exaggeration is ×4.

Figures 9 and 10 show the spot diagrams for rotations about the center of curvature for the off-axis NST telescope. Once again, the secondary mirror is rotated by the same angle and the spot size exaggeration is the same, so these two figures may be directly compared to those in Fig. 5. Since in the parent telescope, center of curvature rotations result in mostly constant coma, we should expect that in the off-axis system, the aberrations will include a little bit of constant coma, a lot of constant astigmatism and some defocus error, according to Table 5. Indeed, Fig. 9a and Fig. 9b show elongated images throughout the field that look like constant astigmatism with a defocus error while Fig. 9c and Fig. 9d show some constant coma. If the two spot diagrams in Fig. 9a and Fig. 9b are refocused, then they also show constant coma (Fig. 10).

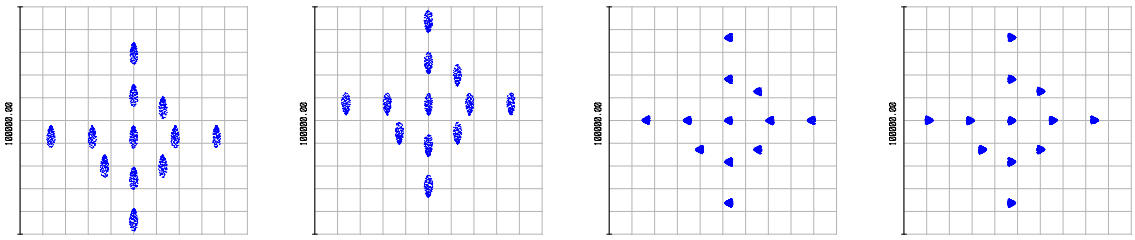

(a) Positive $\vec{x}$ rotation (b) Negative $\vec{x}$ rotation (c) Positive $\vec{y}$ rotation (d) Negative $\vec{y}$ rotation

Figure 9: Spot diagrams when secondary mirror is rotated about its center of curvature by 0.1°. The full field of view is 3 arcminutes. The spot size exaggeration is ×4.

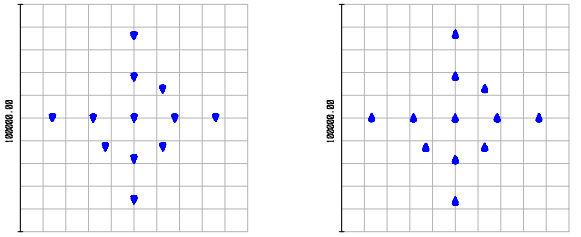

(a) Positive $\vec{x}$ rotation, refocus $= -80.1$ mm

(b) Negative $\vec{x}$ rotation, refocus $= 81.1$ mm

Figure 10: Spot diagrams when secondary mirror is rotated about its center of curvature by 0.1° and images are refocused. The full field of view is 3 arcminutes. The spot size exaggeration is ×4.

4. EFFECT OF MISALIGNMENTS ON POINTING

In some cases, it might be easier to use knowledge of the pointing than to measure the quantity of specific aberrations. To implement this, a laser tracker can be used to align the focal plane to the parent axis of the primary mirror.[14] It is therefore useful to know the amount of the image shift caused by rotation of the secondary mirror. The rotation of M2 about the optical axis and axial translation of M2 in the $\vec{z}$-direction are not considered here because they do not affect the pointing. For this section, we will use the centroid position (for the on axis field point) as the measure of the pointing error in the system. In ZEMAX, the operands CENX and CENY give the x and y coordinates of the centroid in the image plane. Table 6 compares the pointing errors for rotation in both the parent telescope and off-axis NST telescope.

Table 6: Pointing Error (in mm)

Degree of freedom perturbed		Parent		Off-axis	
		CENX	CENY	CENX	CENY
Residual		0	0	0	-0.02
M2 rotation about prime focus	$PFRotX = 1°$	0	-108.0	0	-108.1
	$PFRotY = 1°$	108.0	0	108.0	-0.04
M2 rotation about center of curvature	$CoCRotX = 1°$	0	-11.23	0	-16.02
	$CoCRotY = 1°$	11.23	0	6.53	0.31

For the parent telescope, we observe that rotation of M2 about the coma-free point (prime focus) results in a large pointing error (108 mm), as expected. The other effect of rotation about prime focus in the parent telescope is linear astigmatism (Table 2). Since linear astigmatism in the parent telescope corresponds to linear astigmatism and a plate scale change in the off-axis telescope, no additional pointing errors are expected in the off-axis telescope, and the pointing errors match for the on-axis and off-axis cases.

For rotation about the center of curvature, we observe a small pointing error (11 mm) for the parent telescope. (The pointing error for the CoC rotation in Table 6 is nonzero because the table is recording the centroid pointing, and not the paraxial pointing.) For the off-axis telescope, we expect the pointing errors to be modified from the parent telescope. Since rotation about the CoC results in primarily constant coma (Table 2) for the parent telescope, and this effect translates into a constant tilt (Table 5) for the off-axis telescope, we expect the pointing error to be significantly changed. This is confirmed in Table 6.

5. CONCLUSION

In this paper, we compared the aberrations due to misalignments of the secondary mirror of a rotationally symmetric Gregorian telescope (the "parent telescope") to those of an off-axis version of the same telescope. The degrees of freedom studied were the rotations about the coma-free point (the focus of the primary mirror) and rotations about the center of curvature for the secondary mirror. Rotations about the coma-free point primarily result in both linear astigmatism and pointing errors for the parent telescope while the off-axis telescope includes

the same errors, plus a change in plate scale. Rotations about the center of curvature of the secondary mirror resulted in primarily constant coma and a small amount of linear astigmatism, but no pointing error for the parent telescope. For the off-axis telescope, the constant coma was converted into constant astigmatism, constant tilt (pointing error), and defocus.

6. APPENDIX

The following table provides a comparison of the f/numbers for the NST telescope system and primary mirror for both the actual and parent pupils.

Table 7: NST f/number calculations

Label	$f/\#$	Calculation
NST primary mirror	$f/2.406$	3850/1600
NST system	$f/52.05$	83277.8/1600
Parent primary mirror	$f/0.729$	3850/5280
Parent system	$f/15.77$	83277.8/5280

REFERENCES

[1] Didkovsky, L. V., Kuhn, J. R., and Goode, P. R., "Optical design for a New off-axis 1.7 m Solar Telescope (NST) at Big Bear," *Proc. SPIE* **5171**, 333–343 (2004).

[2] Martin, H. M., Burge, J. H., Miller, S. M., Smith, B. K., Zehnder, R., and Zhao, C., "Manufacture of a 1.7 m prototype of the GMT primary mirror segments," *Proc. SPIE* **6273**, 62730G (2006).

[3] Johns, M., "Progress on the GMT," *Proc. SPIE* **7012**, 70121B (2008).

[4] Wilson, R., [*Reflecting Telescope Optics I: Basic Design Theory and its Historical Development*], Springer (1996).

[5] Schroeder, D., [*Astronomical Optics*], Academic Press (1999).

[6] Mahajan, V., [*Optical Imaging and Aberrations, Part I*], SPIE Press (1998).

[7] Tessieres, R., *Analysis for alignment of optical systems*, Master's thesis, University of Arizona, Tucson, Arizona (2003).

[8] Tessieres, R., Burge, J. H., and Manuel, A. M., "Description of optical aberrations for tilted and decentered systems using Zernike polynomials," Submitted to A.O. (2009).

[9] Thompson, K., *Aberration fields in nonsymmetric optical systems*, PhD thesis, University of Arizona, Tucson, Arizona (1980).

[10] Thompson, K., "Description of the third-order optical aberrations of near-circular pupil optical systems without symmetry," *J. Opt. Soc. Am. A* **22**(7), 1389–1401 (2005).

[11] Tessieres, R., Burge, J. H., and Manuel, A. M., "Alignment of the prime focus corrector," unpublished (2009).

[12] Noll, R., "Zernike polynomials and atmospheric turbulence," *J. Opt. Soc. Am.* **66**(3), 207–211 (1976).

[13] Lundström, L. and Unsbo, P., "Transformation of Zernike coefficients: scaled, translated, and rotated wavefronts with circular and elliptical pupils," *J. Opt. Soc. Am. A* **24**(3), 569–577 (2007).

[14] Burge, J. H., Su, P., Zhao, C., and Zobrist, T., "Use of a commercial laser tracker for optical alignment," *Proc. SPIE* **6676**, 66760E (2007).